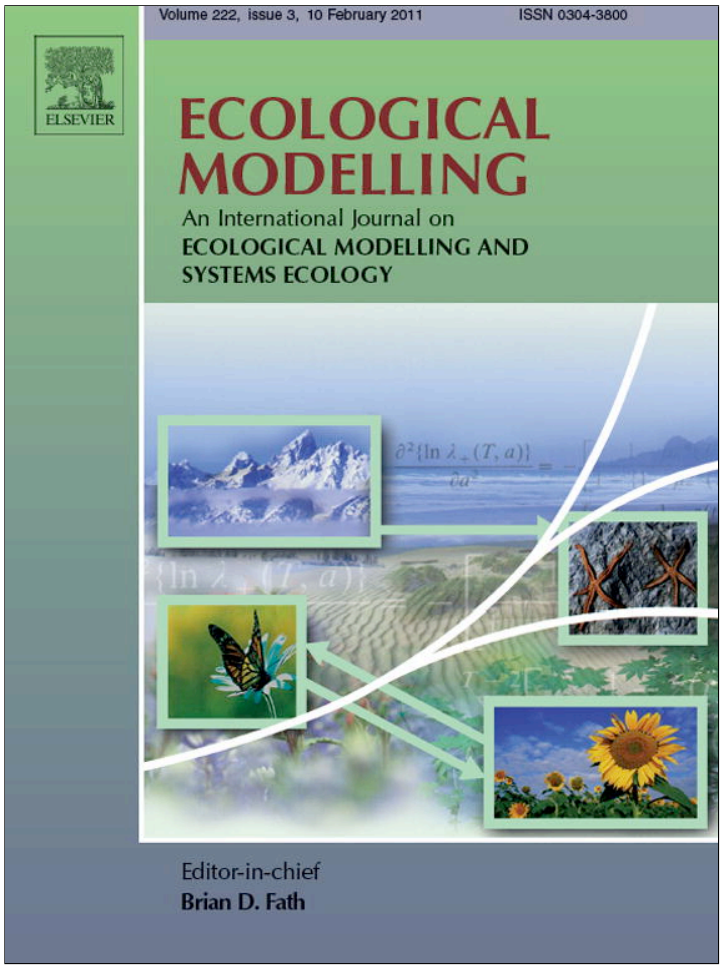

Ecological Modelling 222 (2011) 475–484

Contents lists available at ScienceDirect

Ecological Modelling

journal homepage: www.elsevier.com/locate/ecolmodel

Predicting modes of spatial change from state-and-transition models

Jonathan D. Phillips*

Tobacco Road Research Team, Department of Geography, University of Kentucky, 1457 Patterson Office Tower, Lexington, KY 40506-0027, United States

ARTICLE INFO

Article history:
Received 30 August 2010
Received in revised form
17 November 2010
Accepted 18 November 2010
Available online 16 December 2010

Keywords:
State-and-transition models
Spectral radius
Algebraic connectivity
S-metric
Spatial change
Landscape change

ABSTRACT

State-and-transition models (STMs) can represent many different types of landscape change, from simple gradient-driven transitions to complex, (pseudo-) random patterns. While previous applications of STMs have focused on individual states and transitions, this study addresses broader-scale modes of spatial change based on the entire network of states and transitions. STMs are treated as mathematical graphs, and several metrics from algebraic graph theory are applied—spectral radius, algebraic connectivity, and the *S*-metric. These indicate, respectively, the amplification of environmental change by state transitions, the relative rate of propagation of state changes through the landscape, and the degree of system structural constraints on the spatial propagation of state transitions. The analysis is illustrated by application to the Gualalupe/San Antonio River delta, Texas, with soil types as representations of system states. Concepts of change in deltaic environments are typically based on successional patterns in response to forcings such as sea level change or river inflows. However, results indicate more complex modes of change associated with amplification of changes in system states, relatively rapid spatial propagation of state transitions, and some structural constraints within the system. The implications are that complex, spatially variable state transitions are likely, constrained by local (within-delta) environmental gradients and initial conditions. As in most applications, the STM used in this study is a representation of observed state transitions. While the usual predictive application of STMs is identification of local state changes associated with, e.g., management strategies, the methods presented here show how STMs can be used at a broader scale to identify landscape scale modes of spatial change.

1. Introduction

Environmental changes in landscapes are often spatially complex, due to multiple forcings, spatial heterogeneity of initial conditions, and interactions among components within the landscapes. The purpose of this paper is to introduce methods for identifying the modes of changes in ecosystems and landscapes, as an independent tool for interpreting observed changes, as a guide for the selection of appropriate predictive models, and as a means for predicting modes of change from knowledge of networks of environmental state-changes.

"Mode" has various definitions, but this project is concerned with mode defined as how something happens, or as a particular functioning condition or arrangement. Modes of environmental change are qualitatively different forms, styles, or genres of change. Thus, for example, infiltration-excess or saturation-excess overland flow are different modes of surface runoff generation; and C_3, C_4, and CAM plants represent different modes of carbon fixation.

In the spatial context, modes are characterized by different spatial patterns of change. The response of coastal wetlands to sea-level rise, for example, may be framed in terms of several different modes, from several different perspectives. Geomorphologically, the areal extent of wetlands may increase, decrease, or remain constant depending on the balance between net vertical accretion and coastal submergence. In terms of vegetation communities, transformations could occur along environmental gradients of elevation, salinity, or hydroperiod, with community transitions occurring when critical thresholds are transgressed. Or, transitions could occur in (pseudo-) random patterns as complex interactions among biota, hydrology, geomorphology, and soils create a spatial mosaic, rather than an advancing front, of changes. Conceivably, then, representations of change could be based on linear succession or gradient-type models (e.g., Brinson et al., 1995), random models (c.f. Erfanzadeh et al., 2010), or nonlinear dynamical systems models (e.g., Phillips, 1992).

This study is framed in terms of state-and-transition models (STMs), most commonly used in range ecology (see overviews by Briske et al., 2005; Bestelmeyer et al., 2009), but increasingly applied in ecosystem science more generally (e.g., van der Wal, 2006; Hernstrom et al., 2007; Czembor and Vesk, 2009; Zweig and Kitchens, 2009). Essentially, a STM identifies potential system states, commonly vegetation communities, and the possible transformations among them. The conditions under which these transformations occur are typically further refined based on theo-

* Tel.: +1 859 257 6950.
E-mail address: jdp@uky.edu

0304-3800/$ – see front matter © 2010 Elsevier B.V. All rights reserved.
doi:10.1016/j.ecolmodel.2010.11.018

retical or empirically determined probabilities, or on ecologically based rules or principles. While STMs were conceived as an alternative to classical deterministic succession models, the latter are special cases of STMs, where the state transitions occur in a single linear sequence. Random models are another special case of STM, where transition between any two states is equally likely. Zweig and Kitchens (2009) discuss the application of STMs to address complex succession patterns in wetlands, particularly where multiple stable states are possible.

STMs are typically used to link ecological theory and/or observations to ecosystem management and restoration, or as tools to model, predict, or describe ecological changes based on prior knowledge of processes or phenomena (Bestelmeyer et al., 2009; Zweig and Kitchens, 2009). However, the predictive applications have focused on individual states and transitions. For example, given a particular semi-arid vegetation community, what will be the changes in community composition in response to grazing strategies, fire regimes, or brush control? In this study, the concern is with assessing broader-scale modes of spatial change based on the entire network of states and transitions represented by a STM.

1.1. State-and-transition networks

Ecosystem states and the transitions between them can be treated as a network, with states as the nodes of the network or vertices of the associated graph, and transitions as the links among the nodes. STMs are, indeed, typically represented as box-and-arrow diagrams directly translatable to mathematical graphs. Applications of graph theory in landscape ecology go back to at least the early 1990s (Cantwell and Forman, 1993), and earlier in other aspects of ecology, though the methods are unfamiliar enough to most ecologists that introductions to basic graph theory concepts are still presented in most recent papers (e.g., Tremi et al., 2008; Urban et al., 2009). Previous applications dealt primarily with issues of connectivity and centrality of landscape and habitat elements, and dispersal mechanisms or movement pathways (e.g., Cantwell and Forman, 1993; Bunn et al., 2000; Bode et al., 2008; Tremi et al., 2008; Urban et al., 2009; Padgaham and Webb, 2010). This paper is concerned with the synchronization properties of ecological systems represented as graphs, which has not been studied in landscape ecology or biogeography. Graph theory has also not previously been applied to STMs.

Several end-member or archetypal network structures of STMs can be identified. These provide a template for evaluating the structural connectivity of real-world landscapes and interpreting modes of landscape change. A *linear sequential* STM is a classic succession-type form. For example, in a four-state system with states *A*, *B*, *C*, *D*, *A* leads to *B* leads to *C* and finally to *D* (with reversals possible due to disturbance). A *cyclical sequential* variant may be identified, with state *D* leading back to *A*. Examples of this would include succession where disturbance returns the final state back to *A*. A second case is termed *radiation*. In this case a single state (*A*) can transition to or from any of several states (in this case *B*, *C*, *D*). This could correspond, for example, to a state *A* dominated by a highly successful invading species, whereby invasion of any other state (*B*, *C*, *D*) can result in a transition to *A* (and removal of the non-native may restore *B*, *C*, or *D*). The third extreme is termed *maximum connectivity,* in which all states are linked so that, e.g., *A*, *B*, *C*, or *D* could transition to any of the other states. This is equivalent to a random model, because if any transition is equally possible, then over a broad enough area all will be observed. These archetypes are illustrated in Fig. 1.

Depicting a STM as a network with an associated graph, three metrics are employed here from algebraic graph theory and spectral graph theory (Biggs, 1994) to characterize the modes of spatial

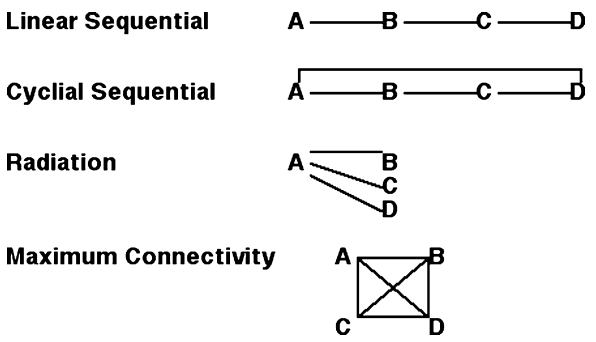

Fig. 1. Archetypal STM network/graph structures for $N = 4$, with system states A, B, C, D.

change. *Spectral radius* is an indicator of the degree of amplification or filtering of changes or perturbations by the system. Fath and colleagues, for instance, have used this measure as an indicator of the intensity of cycling in food webs represented as graphs (Fath, 2007; Fath and Halnes, 2007; Fath et al., 2007). A second metric is *algebraic connectivity*, commonly used as an indicator of the synchronizability of networks (Biggs, 1994). In the context of this study, high levels of synchronization indicate rapid propagation of effects through the spatial network (and vice versa). The *S-metric* was derived by Li et al. (2005) as an indication of the extent to which a system is scale-free. The index is sensitive to the degree to which network nodes are hubs with multiple links. In the context of this study the *S*-metric is an indication of (system) structural constrains on state transitions. These metrics will be discussed further below.

1.2. Spectral radius

Each STM can be considered as a network represented by a graph with *N* nodes (the states) and *m* edges or links (transitions between states). These graphs may be directed (transitions are only possible in one direction along any edge) or undirected (transitions are possible in both directions). Undirected graphs will be considered here, as most STMs allow two-way transitions among pairs of states. Graphs are connected if it is possible to follow a path of one or more edges between any two nodes. Any graph has a $N \times N$ adjacency matrix *A*, the entries of which are 1 if the row and column states or nodes are connected, and zero otherwise. For the case of an undirected, connected graph *A* is symmetric. The adjacency matrix has *N* eigenvalues λ, which may be complex numbers, the real parts of which are ordered such that $\lambda_1 > \lambda_2 \ldots > \lambda_{N-1} > \lambda_N$. The largest eigenvalue is the spectral radius, and λ_1 is an important determinant of many system properties (Restrepo et al., 2007). The spectral radius is directly related to the number of paths or cycles in a network. $\lambda_1 < 1$ indicates damping or filtering behavior, so that changes are essentially absorbed by the system. If $\lambda_1 > 1$ amplification effects are indicated, with higher values indicating stronger amplification.

The maximum spectral radius for a graph of a given number of nodes or states and edges or transitions is

$$\lambda_{1,\max} = \left[2m\frac{(N-1)}{N}\right]^{0.5} \quad (1)$$

Based on this, maximum λ_1 for the archetypal STM structures can be determined as follows:

Linear sequential, radiation: $\lambda_{1,max} = [2(N-1)^2/N]^{0.5}$
Cyclical sequential: $\lambda_{1,max} = [(2N)(N-1)N^{-1}]^{0.5}$
Maximum connectivity: $\lambda_1 = \lambda_{1,max} = N-1$

Using λ_1, λ_{upper}, λ_{max}, respectively, to signify the observed largest eigenvalue, the upper bound on λ_1 for given N and m, and the upper bound for a given N (Phillips, in press):

$$\frac{\zeta_{connection}}{\zeta_{total}} = \frac{(\lambda_{max} - \lambda_{upper})}{(\lambda_{max} - \lambda_1)} \quad (2)$$

$$\frac{\zeta_{wiring}}{\zeta_{total}} = 1 - \frac{\zeta_{connection}}{\zeta_{total}} \quad (3)$$

The contribution to reduction of λ_1 associated with having fewer transitions or edges than the maximum connectivity or random case is given by $\zeta_{connection}/\zeta_{total}$. The relative importance of the specific network of connections (i.e., how a given number of nodes are linked given a specific m) or "wiring" is indicated by $\zeta_{wiring}/\zeta_{total}$.

1.3. Algebraic connectivity

Algebraic connectivity is defined as the second-smallest eigenvalue (λ_{N-1}) of the Laplacian matrix $L(A)$ of the adjacency matrix. The entries of $L(A)$ are:

$$a_{ij} = \begin{cases} deg(v_i) & \text{if } i = j \\ -1 & \text{if } i \neq j \text{ and } v_i \text{ adjacent to } v_j \\ 0 & \text{otherwise} \end{cases}$$

where $\deg(v_i)$ is the degree of vertex or node i. The degree is equal to the number of transitions or edges connected a node to other nodes.

Algebraic connectivity (λ_{N-1}) is a measure of the synchronizability of the system (Biggs, 1994; Duan et al., 2009), and is bounded by the vertex connectivity $\kappa(A)$ and graph diameter D:

$$\frac{4}{ND} \leq \lambda_{N-1} \leq \kappa(\mathrm{A}) \quad (4)$$

Vertex connectivity is the minimum number of vertices or nodes that could be removed to disconnect the graph. D is the maximum shortest path (number of links or edges) between any two vertices. Vertex connectivity is bounded by edge connectivity of A such that $\kappa(A) \leq$ edge connectivity $\leq$ minimum degree. Edge connectivity is the minimum number of edges that could be removed to disconnect the graph. Minimum degree is the smallest number of edges associated with any node or vertex.

Vertex connectivity for the sequential and radiation archetypes is *1*, while $k(A) = N-1$ for the maximum connectivity case. $D = N-1$ for the linear sequential and $N-2$ for the cyclical sequential cases. For the radiation type, $D = 2$, and $D = 1$ for maximum connectivity. Thus the following intervals can be defined for algebraic connectivity:

linear sequential: $4/(N^2 - N) \leq \lambda_{N-1} \leq 1$
cyclical sequential: $4/(N^2 - 2N) \leq \lambda_{N-1} \leq 1$
radiation: $4/(2N) \leq \lambda_{N-1} \leq 1$
maximum connectivity: $4/N \leq \lambda_{N-1} \leq N - 1$

1.4. S-metric

The S-metric $s(g)$ devised by Li et al. (2005) applies to undirected, simple, connected graphs with a fixed degree sequence:

$$s(g) = \sum_{i=1}^{(N-1)} (d_i d_{i+1}) \quad (5)$$

where d is the degree of a given node or state (these appear as the diagonal elements of the Laplacian). By arranging the adjacency matrix in order of increasing or decreasing degree, the fixed degree sequence requirement can be met. The S-metric measures the extent to which g has a hub-like core. Maximum $s(g)$ values occur when high-degree nodes are connected to other high-degree nodes. Further comments on the mathematical developments and implications are given by Li et al. (2005).

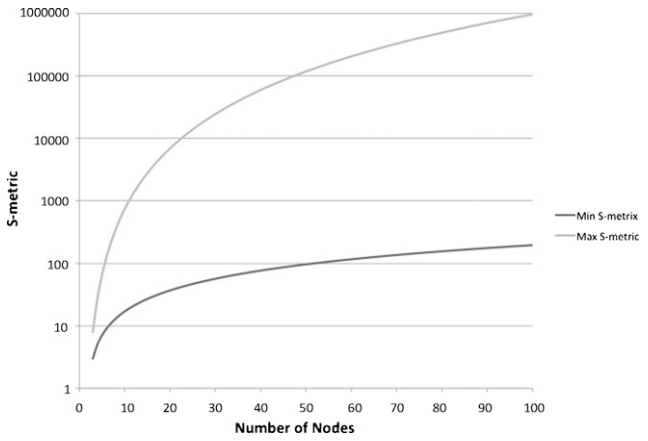

Fig. 2. Minimum and maximum S-metric values, for systems with three to 100 states.

For the archetypal cases:

linear sequential: $s(g) = \left\{ \sum_{i=1}^{N-1} \left[(i-1)N - (i-1)^2 \right] \right\} - N$
cyclical sequential: $s(g) = \sum_{i=1}^{N-1} \left[(i-1)N - (i-1)^2 \right]$
radiation: $s(g) = (N-1) + (N-2)$
maximum connectivity: $s(g) = (N-1)^3$

The application of spectral radius, algebraic connectivity, and the S-metric is illustrated below.

2. Applications and interpretations

2.1. Modes of environmental change

Spectral radius, algebraic connectivity, and the S-metric are interrelated and not independent. Highly connected STMs, for instance, will have higher values of all three. They do, however, have different sensitivities to various aspects of network structure, and capture different aspects of spatial landscape response.

The spectral radius is most strongly influenced by the connectivity within the system. STMs where state transitions could be propagated indefinitely throughout the system without reaching dead ends will yield high λ_1 values, while those with more limited propagation produce lower λ_1. Higher λ_1 indicate greater potential amplification of a change signal in the landscape. Algebraic connectivity is well established as an index of synchronization in graphs and networks. In the context of spatial landscape change, higher algebraic connectivity suggests that changes can ripple more rapidly through the ecological system, and vice versa. System structural constraints to change (i.e., chains of transitions through the landscape) will be reflected in lower S-metrics, and limited constraints by higher values. The response of these measures to variations in STM structure is explored below.

2.2. Variation and sensitivity

2.2.1. Spectral radius

As illustrated by Eq. (1), the maximum λ_1 can be determined for a graph of any given N, m, as a nonlinear square root function. For a given number of nodes, $m = N\times$ (mean degree of nodes). Varying m by a factor of *9* only produces a $\sim 3\times$ change in spectral radius. The figure shows a greater sensitivity at the low end, but also shows

that the spectral radius increase is disproportionately small relative to *N*.

Spectral radius is *relatively* more sensitive to the "wiring" of the system than to the number of transitions. Eqs. (2) and (3) show, for example, that for any case other than $\lambda_1 = \lambda_{upper}$, reduction of the observed spectral radius relative to λ_{max} is less than that associated with *m* less than the maximum connectivity case.

2.2.2. Algebraic connectivity

Eq. (4) shows that the upper bound on algebraic connectivity is linearly related to the vertex connectivity, and therefore to the minimum degree. For the type of STMs and graphs considered here, it is strongly constrained to ≤ 1. In general, the upper bound on algebraic connectivity is constrained by the "weakest link" in terms of the system state with the fewest transitions to other states.

For a given *N* the lower bound of algebraic connectivity is a nonlinear function of graph diameter, with a decrease in minimum algebraic connectivity as graph diameter increases. The function decreases rapidly as *D* increases from the minimum of *1* (for any graph) but more slowly as *D* approaches the maximum of $N - 1$ for any connected graph. Algebraic connectivity is thus strongly sensitive to small deviations from the maximum connectivity case, and less sensitive to increasingly larger path distances (number of state transitions) between the most separated states.

2.2.3. S-metric

For a given number of states in a connected graph, the minimum $s(g)$ is associated with a radiation type structure, where $s(g) = (N-1) + (N-2)$. The maximum occurs for the maximum connectivity case, where $s(g)$ varies as the cube of $N - 1$. Fig. 2 plots the maximum and minimum *S*-metrics for $N = 3$ to 100. Both minimum and maximum $s(g)$ increase very rapidly with *N* up to about 10, and less rapidly, but still quite strongly, for larger STMs (note the logarithmic vertical axis). The *S*-metric is thus highly sensitive to system size, especially at the lower end. Note also the increase in $s(g)_{max} - s(g)_{min}$ with *N*. This shows that the potential variation in the *S*-metric is increasingly sensitive to the transition structure at larger *N*.

In general, the discussion above shows that the spectral radius is disproportionately insensitive to the number of states and transitions, and more sensitive to the number of cycles and transition loops (state transition sequences that may start and end in the same state). The algebraic connectivity is most sensitive to the system state(s) least prone to transition, and thus to potential buffers or bottlenecks to spatial propagation of changes within the landscape. The *S*-metric is strongly affected by the number of states, and for a given *N*, is increasingly sensitive to the number and magnitude of highly connected nodes at larger *N*.

2.3. Modes and metrics

Successional or gradient-driven landscape change would thus be characterized by STMs with the lowest spectral radius and algebraic connectivity relative to *N*, with low *S*-metrics as well. Radiation-type change will be characterized by higher spectral radia and algebraic connectivity than the sequential modes, but the major signature is the *S*-metric, which should be at or near the minimum. The closer a STM is to a random or pseudo-random structure where any transition between any two states is possible, the closer all the metrics will be to their maximum values.

The metrics are also capable of identifying modes other than the archetypes. For instance, a landscape where change is facilitated by a relatively high number of hub-type nodes (states with multiple possible transitions), but also limited by at least one state with minimal transition connectivity, would be characterized by a relatively high *S*-metric and relatively low algebraic connectivity. Where a single state is disproportionately important as a hub (many possible transitions), the *S*-metric will be low. Where hub-like structure is limited but many cyclic transition sequences exist, spectral radius will be high and the *S*-metric relatively low.

STMs in the literature, as well as the example below, are generally $N < 10$. As mentioned above, spectral radius is more sensitive to changes in system size at lower *N* than at higher *N*. The *S*-metric, by contrast, shows greater spread and thus greater potential discriminatory power, at higher *N* (though, again, note the logarithmic *x*-axis of Fig. 4).

3. Guadalupe/San Antonio River Delta

This study uses soil types in the Guadalupe-San Antonio River delta (GSARD) of Texas to represent system states. The case study was conducted in the context of a broader study of the effects of fluvial geomorphic changes (particularly channel shifts or avulsions, lateral channel migration, and meander cutoffs), coastal submergence due to a combination of sea-level rise and land subsidence, changes in freshwater inflow due to climate change and water diversions and withdrawals, and hydrologic modifications (ditches, canals, levees, etc.).

Soils represent the combined, interacting influences of climate, biota, topography, hydrology, geology or parent material, and age or stability of land surfaces. In the study area soil types represent different combinations of substrates, related to depositional environments; topographic settings, reflected in soil drainage and other properties and related to geomorphic processes and changes in the fluviodeltaic system; soil chemistry, linked to influences of saltwater and to parent material chemistry; and the age and stability of the geomorphic surfaces they occupy. At least three important gradients occur—a saltwater–freshwater gradient from Guadalupe Bay upstream into the delta heads, local elevation gradients that largely control soil drainage and moisture, and age gradients of geomorphic surfaces. The ecological significance of the soils as system states is reflected in the fact that they are assigned different ecological site ratings or designations in the U.S. soil survey system (Bestelmeyer et al., 2009; NRCS, 2010). The study area soils will be discussed further in the results section.

3.1. Conceptual models of deltaic change

At least three different conceptual frameworks of landscape change are relevant to the GSARD. One is derived from the geomorphology and sedimentology of deltas, and is based on systematic changes in geomorphic processes and sedimentary processes as deltas prograde, erode, or are transgressed by rising sea level. In the vertical dimension, stratigraphy represents successional sequences of sedimentary layers and packages. In the horizontal dimension, topography and surficial materials represent a gradient of relative importance of fluvial vs. coastal/tidal influences. These conceptual models are described in most modern sedimentology and sequence stratigraphy texts, and Anderson and Rodriguez (2008) give examples of specific sequences for deltas on the Gulf of Mexico coast. Second, studies of wetland response to rising sea level have identified sequences of soils and associated vegetation along gradients of elevation, hydroperiod, and salinity (e.g., Brinson et al., 1995; Gardner and Porter, 2001).

A third conceptual framework comes from river science, based on general upstream–downstream and cross-valley environmental gradients overlaid by local spatial variations and modified by geomorphological, hydrological, and ecological interactions to produce, e.g., river styles or functional process zones (Brierly and Fryirs, 2005; Thorp et al., 2008). This implies cross-valley environmental gradients superimposed on down-valley gradients, with additional local spatial variability imposed on both sets of gradi-

ents by environmental heterogeneity independent of the cross- and down-valley gradients.

The conceptual frameworks derived from river science imply a sort of constrained self-organization, in the sense of emergent system states influenced by a hierarchy of environmental controls or gradients. The other frameworks above call for systematic, succession-type changes along environmental gradients. However, the delta stratigraphic framework applies to relatively long temporal scales, broad spatial scales, and highly generalized characterizations of system state. The wetland response framework is applicable at more detailed spatial scales and environmental state characterizations, but applies only near the leading edge of externally driven changes.

These frameworks (and others that might be brought to bear) are not mutually exclusive or competing, and the STM analysis is not intended to distinguish among them. Rather, the point is that relevant and well-tested conceptual models of environmental change do not necessarily indicate the mode of landscape-scale spatial change. This can be accomplished, however, by examining the network of state transitions via the spectral radius, algebraic connectivity, and *S*-metric.

3.2. Study area

The Guadalupe River, Texas, rises in the hill country of the Edwards Plateau, west of the Austin-San Antonio corridor, and has a drainage area of about 27,000 km^2. The Guadalupe crosses the Balcones Escarpment marking the southeastern margin of the Edwards Plateau, and the Gulf of Mexico Coastal Plain before discharging into Guadalupe Bay, part of the San Antonio Bay estuary. About 11 km upstream of the bay, the Guadalupe is joined by the San Antonio River, which rises near the city of San Antonio. The study area (Fig. 3) includes the deltas of both rivers.

The Holocene development of the GSARD is described by Donaldson et al. (1970), Ricklis and Blum (1997), and Weistein and Black (2009). Like other Gulf of Mexico rivers, the lower San Antonio and Guadalupe Rivers have been profoundly influenced by sea level change. Throughout the Quaternary a series of valley incision episodes during colder climates and lower sea-levels have alternated with aggradation during rising sea-level, creating a system of alluvial terraces within the river valleys, which are themselves cut into the older, Pleistocene Beaumont terrace. Sea-level has generally been rising throughout the Holocene.

Beyond the climate and sea-level driven changes, and associated Holocene vegetation change, the GSARD is characterized by numerous channel shifts (avulsions), lateral channel migration, and meander cutoffs, all of which are common in deltas and coastal plain alluvial rivers. In addition to these natural changes, since the 1830s the delta has been subject to a number of human modifications, including construction of numerous levees and drainage ditches and canals, water withdrawals upstream, water diversions within the delta area, and oil and gas production. The predominant land use, other than some areas set aside as part of a wildlife refuge, is grazing. Oil and gas production occurs generally within the rangelands.

3.3. Delta soils

Soil series mapped in the study area are differentiated by several criteria related directly to geomorphic processes, Holocene deltaic evolution, age or stability of alluvial landforms, and local edaphic conditions. These include:

- presence or absence of mollic epipedons, which in this environment develop in wetlands influenced by salt or brackish water flooding;
- clay mineralogy, related to depositional environment and sediment source;
- acidity and alkalinity, linked to proximity to salt water and soil drainage;
- soil drainage, controlled by elevation and distance from active channels;
- soil texture, related to depositional environments.

Transitions among soil types can therefore be linked to

(1) changes in relative sea level, which affect salinity, soil drainage, and alluvial depositional environments;
(2) local channel incision/aggradation, which affects soil drainage and frequency and duration of inundation;
(3) avulsions and cutoffs, which modify (and locally create new) depositional environments, and influence frequency and duration of inundation;
(4) lateral channel migration, affecting depositional environments and frequency and duration of inundation;
(5) floodplain surface aggradation, which affects surface texture and soil drainage and frequency and duration of inundation;
(6) age and geomorphic stability of surfaces, which determines the potential expression of pedogenic features such as cambic or argillic horizons;
(7) artificial levees and channels, which may influence drainage, frequency and duration of inundation, depositional environments, and deposition rates and types.

Beyond the direct impacts of item (7), all of the above may be indirectly influenced by human agency. The soil taxa found are discussed in Section 4.

The soil series are associated with specific ecological site characteristics in the soil survey database. In some cases these ecological sites are associated with identified state transitions in vegetation communities, often involving savannah, grassed woodland, woodland, and invaded grassland states. The identified transitions between them are associated with various combinations of grazing regimes, brush management, and fire regimes (NRCS, 2010; USDA, 2010). The focus in this study is on transitions among the soil types, reflecting the geomorphic and hydrologic changes mentioned above, rather than vegetation community transitions associated with range management.

3.4. Methods

Soil series mapped in the delta were inventoried through the U.S. Department of Agriculture Web Soil Survey (http://websoilsurvey.nrcs.usda.gov/app/HomePage.htm). Possible transitions were based on three criteria, applied sequentially:

(1) The soils are spatially adjacent at some location within the study area.
(2) The soils are geographically related, in that local differences in, e.g., elevation, result in local juxtaposition of the soil types. This was determined from the soil survey reports of the two counties in the study area, Victoria and Refugio (Miller, 1982; Guckian, 1986). If two of the mapped series are both included in a broader-scale soil association, or if one soil was listed as an inclusion in the mapping unit description of another, then they were considered geographically related. The standards for defining soil associations, and for describing mapping units and their inclusions, are spelled out in Soil Survey Division Staff (1993) and USDA (2010).
(3) Plausible genetic linkages exist between the soil, in the sense that one series could be converted to another by, e.g., erosion

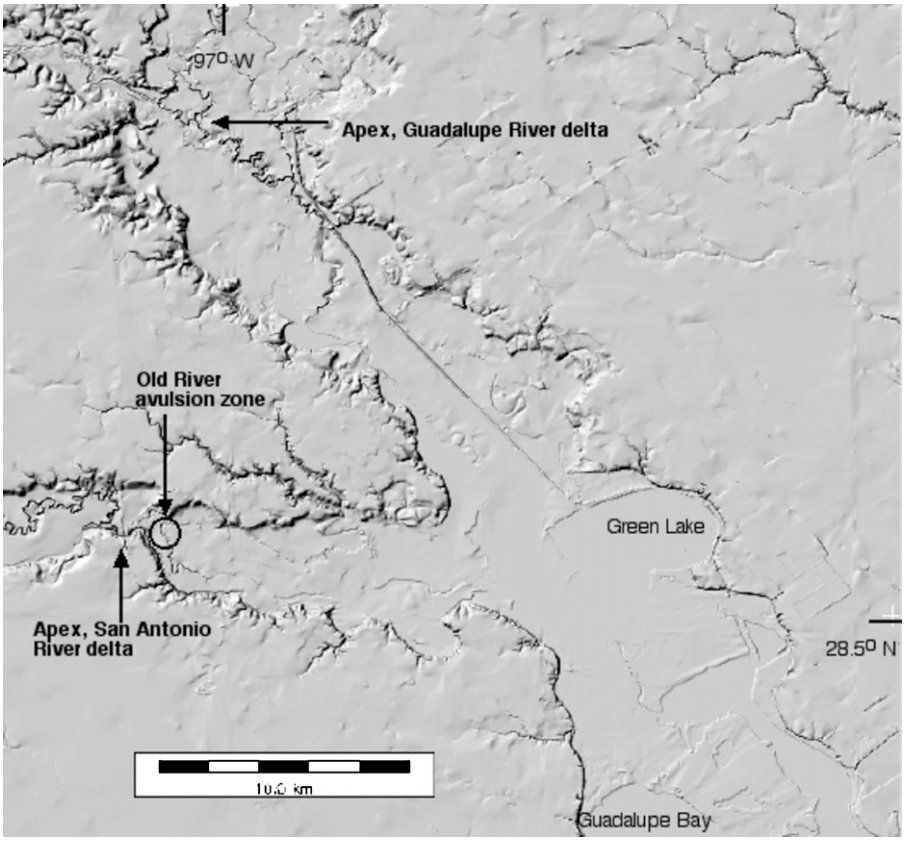

Fig. 3. Study area map, shown as a shaded relief map derived from 30-m resolution digital elevation data.

or deposition, or improved or impeded soil drainage. This was based on extensive field observations in the area in connection with a study on historical changes in water and sediment fluxes (Phillips, 2010).

An adjacency matrix of these series was constructed, with cell values of *1* if the soils are potentially transitional to each other, and zero otherwise. The spectral radius, algebraic connectivity, and *S*-matrix were calculated as described earlier. As nine soil types were found, values of these parameters for the archetypical STMs were also calculated for $N = 9$.

4. Results

4.1. Delta soils and transitions

The nine soils mapped in the GSARD area are shown in Table 1. The Aransas, Austwell, and Trinity series represent a catenary gradient of influence by brackish or saltwater flooding in the lower delta, with the series, respectively, representing slightly higher elevation or more upstream positions. The Placedo series occupies infilled or infilling abandoned channels in the same area. Transitions among these soils may thus be associated with coastal submergence, changes in freshwater inflow, local topographic change due to deposition and surface scour, and avulsions or cutoffs. Note that the mollic epipedons of the Aransas (and Degola) series do not necessarily connote geomorphic stability, but rather the accumulation of organic matter in a wetland environment, with high base status provided by both salinity and calcareous sedimentary parent material.

The Degola, Meguin, and Rydolph are floodplain soils in the middle and upper delta, either upstream of the group mentioned above, or on portions of the floodplain further removed from the main

Table 1
Soils of the Guadalupe/San Antonio River delta.

Soil	Taxonomy[a]	Geomorphic interpretation
Aransas	Fine, montmorillonitic (calcareous), hyperthermic Vertic Haplaquolls	Low floodplain surfaces in lower deltatic fluvial-estuarine transition zone; influenced by saltwater inundation
Austwell	Fine, montmorillonitic (calcareous), hyperthermic Typic Haplaquepts	Low floodplain surfaces in lower delta; occasionally influenced by saltwater inundation
Degola[b]	Fine-loamy, mixed, hyperthermic Cumulic Haplustolls	Natural levees & convex ridges on slowly accreting floodplain surfaces
Meguin	Fine-silty, mixed, hyperthermic Fluventic Haplustolls	Stable or slowly accreting flat or slightly convex surfaces on inner portions of active floodplain
Placedo	Fine, montmorillonitic, nonacid, hyperthermic Typic Fluvaquents	Infilled or partly infilled paleochanels, lower delta
Rydolph	Fine-silty, mixed (calcareous), hyperthermic Aeric Fluvaquents	Recent, actively accreting floodplains, upper delta
Sinton	Fine-loamy, mixed, hyperthermic Cumulic Haplustolls	Channel belts abandoned by avulsions; crevasse fillings
Trinity	Very-fine, montmorillonitic, thermic Typic Pelluderts	Low, relatively stable floodplain surfaces on clayey overbank & channel fill deposits
Zalco	Sandy, siliceous, hyperthermic Typic Udifluvents	Recent sandy fluvial channel and point bar deposits, upper delta

[a] U.S. Soil Taxonomy.
[b] Some pedons are taxadjuncts, with more alkaline/calcarous subsoils than is typical for the series.

Table 2
Adjacency matrix.

	Aransas	Degola	Sinton	Austwell	Placedo	Meguin	Trinity	Rydolph	Zalco
Aransas	0	1	1	1	1	0	1	1	0
Degola	1	0	0	0	0	1	0	0	0
Sinton	1	0	0	0	0	1	1	0	1
Austwell	1	0	0	0	1	0	1	1	0
Placedo	1	0	0	1	0	0	1	0	0
Meguin	0	1	1	0	0	0	1	1	1
Trinity	1	0	1	1	1	1	0	1	0
Rydolph	1	0	0	1	0	1	1	0	0
Zalco	0	0	1	0	0	1	0	0	0

active channel(s). The differences between them are based on subtle elevation and topographic differences, reflected in significant differences in clay content. There is enough input of silt (or silt content of the parent material) to keep them out of the montmorillonitic families that include the Aransas, Austwell, Placedo, and Trinity series. Transitions among these can be caused by local topographic change due to deposition and surface scour, and changes in depositional environments associated with lateral channel migration, avulsions, or cutoffs.

The Sinton series is interpreted by the U.S. Department of Agricultural soil survey program, in both the official series descriptions database and in the local soil surveys (Miller, 1982; Guckian, 1986), as occupying crevasse fills. However, fieldwork for this study found that all large delineations of the Sinton series actually occupy former channel belts abandoned by avulsions, with most of the latter occurring in the past 200 years (Phillips, 2010). The Zalco series is poorly developed and sandy and occurs on coarse recent deposits. The San Antonio River delta is fine-grained throughout. The Zalco is not mapped in that portion of the delta, and no sufficiently coarse deposits to potentially develop this soil type were observed. Thus the Zalco series is confined to point bar and channel deposits in the upper portion of the Guadalupe River delta.

Transitions between the lower delta and upper/middle delta groups of soils can occur due to coastal submergence or changes in freshwater inflow, or avulsions that transcend the upper/middle and lower delta. The Sinton series could be transformed by various combinations of burial, inundation, and reoccupation of former channel belts; or created from other soils by new avulsions. Stabilization of deposits hosting the Zalco series, with additions of fine material, could result in transitions to the Degola, Meguin, or (most likely) Rydolph series. Lateral channel migration or high-flow slugs of coarse alluvium can create new Zalco locations.

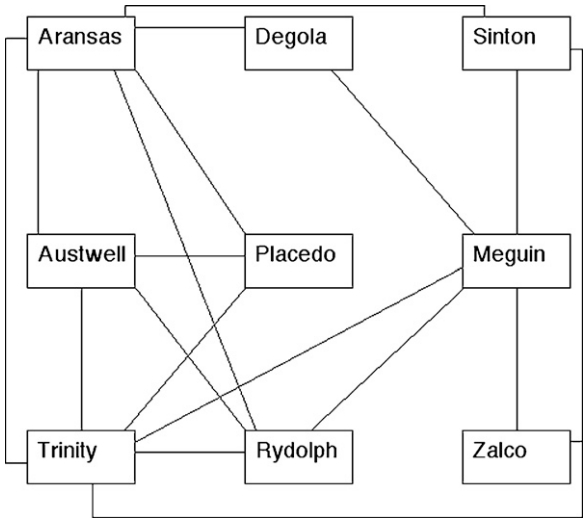

Fig. 4. State-and-transition model for soils of the Guadalupe/San Antonio River delta.

Table 3
Results for study area (observed) compared with archetypal structures of a network of similar size.

	Spectral radius	Algebraic connectivity	*S*-metric
Linear sequential	1.902[a] 3.771[b]	$0.056 \leq \lambda_{N-1} \leq 1$	27
Cyclic sequential	2.000[a] 3.771[b]	$0.063 \leq \lambda_{N-1} \leq 1$	32
Radiation	2.828[a] 4.000[b]	$0.222 \leq \lambda_{N-1} \leq 1$	15
Max connectivity	8.000	$0.444 \leq \lambda_{N-1} \leq 8$	512
Observed	4.428	1.402	140

[a] Computed values assuming a starting point of the first state in the adjacency matrix.
[b] Maximum upper bound of λ_1 for $N = 9$.

4.2. STM analysis

The adjacency matrix is shown in Table 2, and a graphic version of the STM in Fig. 4. The spectral radius is 4.428, algebraic connectivity is 1.402, and the *S*-metric is 140. These are compared with the values for the archetype configurations in Table 3. The observed values for spectral radius, algebraic connectivity, and *S*-metric relative to those for the archetype STM structures are shown graphically in Fig. 5.

$\zeta_{connection}/\zeta_{total} = 0.656$, and $\zeta_{wiring}/\zeta_{total} = 0.344$, indicating that about two thirds of the reduction in spectral radius from that associated with a fully random, maximum-connection extreme is associated with a reduction in the number of edges or transitions from 36 to 18. About a third is due to the specific arrangement of connections.

4.3. Model validation

An avulsion occurred near the upper end of the San Antonio River delta some time after 1930, when the major course switched from what is shown on maps as the Old River channel to the modern river course (Phillips, 2010). At the time of soil mapping, the Old River channel was still functioning as an anabranch of the San Antonio River, as shown by the aerial photographic base for the soil

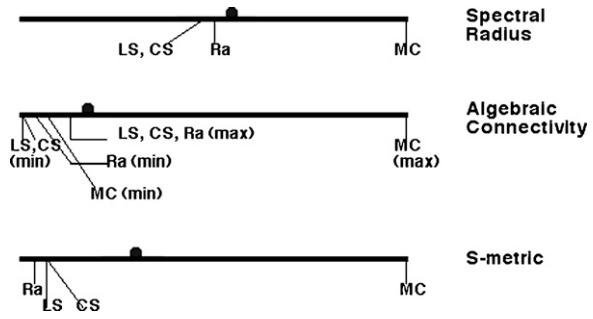

Fig. 5. Observed values for key metrics (large dots) relative to those for archetypal structures. Each bar is scaled to represent zero to the maximum possible value for $N = 9$. LS = linear sequential; CS = cyclical sequential; Ra = radiation; MC = maximum connectivity.

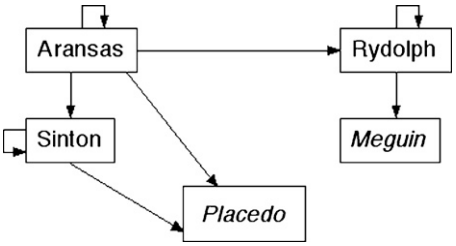

Fig. 6. Soil transitions in the Old River avulsion zone following abandonment of the Old River channel. Self-referencing arrows represent persistence of some areas of existing soil types. New soil series in the zone are indicated in italics.

maps, and other aerial photographs as recent as the late 1990s. By the time of field work in 2010, the Old River channel had infilled to the point that it does not convey flow except during floods. Pedologic changes in the Old River avulsion zone (see Fig. 3) were evaluated to determine the extent to which they conform to the STM analysis. Because these observations were not used to construct the STM model in Fig. 4, this constitutes validation in sense of Urban et al. (2009).

The soil maps show this portion of the delta to be occupied by the Aransas, Rydolph, and Sinton series, though the mapped areas of Aransas probably derive their base status from calcareous material rather than salinity. In some mapped zones of Aransas and Sinton soils, areas of the Placedo series have appeared as the Old River and its tributary channels infill. Changes in sedimentation patterns near the avulsion site have also converted some areas mapped as Aransas to the Sinton series, where cumulic epipedons have developed on the abandoned meander belt, or the Rydolph where active floodplain sedimentation is now concentrated. Some formerly actively accreting units of the Rydolph series have developed mollic layers and transformed to the Meguin series as the surfaces stabilize.

These transitions are shown in Fig. 6, where the Aransas, Rydolph and Sinton series persist in part, and partly transition to other soils. Two soils previously absent (or at least unrecognized), the Meguin and Placedo series, have developed. Five different soil transitions occur for the three pre-existing soil types. One series (Aransas) has been transformed into three other soil types, and one of the previously absent series (Placedo) has developed from two different "parent" soils.

As discussed more fully below, the spectral radius of the STM indicates relatively rapid, complex modes of change, with general amplification of effects and increasing spatial complexity, which is evident in Fig. 6. Algebraic connectivity is higher than for sequential or radiation structures, but much lower than for a maximum-connectivity case, reflecting the role of local environmental gradients. The Old River avulsion zone results are generally consistent with this implication, as most transitions are related to increases or decreases in sedimentation and stabilization of geomorphic surfaces. The *S*-metric indicates significant structural constraints in the propagation of state transitions, which is also consistent with the validation results. All but one (Aransas-to-Placedo) of the observed transitions in the Old River avulsion zone is present in the STM model shown in Fig. 4.

5. Discussion

The observed spectral radius is more than double those for sequential configurations, and > 1.5 times that of a radiation model. The spectral radius for the GSARD soil graph is more than half the maximum possible value for a nine-state system. This indicates more rapid and complex spatial landscape transitions than would be predicted or successfully modeled by successional, sequential, or cyclical models, or by radiation to or from a single key component. All the configurations predict amplification of changes rather than damping, and the measured $\lambda_1 = 4.428$ is indicative of strong amplification, suggesting that changes driven by, e.g., sea-level rise, reduced freshwater inflow, or channel shifts would have knock-on effects throughout the delta.

The maximum possible values for λ_1 and algebraic connectivity are associated with the maximum connectivity case. The observed spectral radius of about 4.4 is 80% lower than that for the maximum connectivity case. This indicates a complex but nonrandom spatial transformation, constrained by "rules" such as the absence of Zalco in the San Antonio River delta, the association of Sinton with avulsions, and the "taxonomic distance" between some series (e.g., Aransas and Meguin) which would require geomorphic changes through one or more intermediary states.

The observed algebraic connectivity is more than six-fold lower than for the maximum connectivity case, reflecting the fact that transitions are possible, or at least more probable, along gradients of, e.g., elevation, saltwater influence, and geomorphic age. Thus the synchronizability is much lower than for a fully connected, random case.

The *S*-metric is an order of magnitude higher than that of the sequential and radiation forms. The value much lower than that for the maximum-connectivity case indicates that there are significant structural constraints on propagation of responses within the system.

In the GSARD, results indicate that external drivers of change such as, e.g., coastal submergence from the bay and lower delta, or changes in fluvial water or sediment inputs from the upper delta, will not result in a mode of change characterized by relatively simple spatial translation along environment gradients, nor by convergent state transitions. Rather, results suggest a complex pattern of state transitions throughout the delta, with multiple local and overall possibilities, and controlled by localized rather than delta-wide environmental gradients. Results also suggest that drivers of change within the delta, such as a water control structure or a meander cutoff, may trigger chains of state transitions. Land managers planning for sea-level rise, or water resource managers exploring potential impacts of upstream withdrawals or diversions, for example, should thus not expect an advancing wave of state transitions, but a complex, spatially variable mosaic of change.

Because the STM is based on observed spatial adjacencies and change indicators, errors of commission (inclusion of transitions which can or do not happen) cannot occur unless the empirical observations are erroneous. However, as the validation test in the Old River avulsion zone shows, errors of omission may occur. This suggests that, where confidence in the observations underlying an STM is high, any errors in λ_1, algebraic connectivity, or $s(g)$ are likely to be underestimates. This is because errors of omission undercount m, and all three parameters increase, other things being equal, as the number of links or edges increases.

In some cases the structure of a graph or STM is visually evident when the pattern is (or is close to) one of the archetypal structures such as the examples in Fig. 1, canonical graphs analyzed in the mathematical literature (see, e.g., Biggs, 1994) or other common configurations such as those related to landscape connectivity structures outlined by Cantwell and Forman (1993). In other cases the extent to which an STM represents—or deviates from—sequential, radiation, or random structures is not obvious from visual inspection. The situation is analogous to that of an *x*-*y* scatterplot—in some cases the relationship is easily recognized visually, but in other cases regression measures are necessary to characterize the nature of the relationship, and in any case are useful for quantification thereof.

Three objectives in introducing these methods for identifying the modes of changes in ecosystems and landscapes were out-

lined in the introduction: a tool for interpreting changes, a guide for the selection of appropriate predictive models, and a means for predicting modes of change from knowledge of networks of environmental state-changes. These may be illustrated using the GSARD case study. Observations of divergent development of soils, landforms, or ecosystems, or habitat fragmentation, would be interpreted according the STM analysis as an expected outcome rather than an exceptional case. By the same token, observations of monotonic sequential changes would be interpreted as an exceptional case (in a case such as this where confidence in the STM is high), not likely to persist or recur.

The STM analysis would suggest use or development of predictive models that can accommodate multiple pathways and outcomes. This, in turn, points to, e.g., river styles or functional process zone conceptual models rather than sequence stratigraphic or river continuum frameworks for geomorphology; full implementation of soil-landscape or state factor models (in preference to simplified catenary or chronosequence relationships) for soils; and plant community STMs (like those used for rangeland communities in south Texas) instead of linear successional models for vegetation.

At this point, and in this example application, predictions produced by the STM analysis are qualitative and imprecise, as outlined above. In the GSARD, for instance, results predict that an avulsion is likely to trigger a complex chain of responses, but that responses will not be synchronous. The direct predictive power of the analysis is thus relatively small. However, by conducting similar assessments of other STMs, insight can be gained into how individual local environmental state transitions are translated to the landscape scale.

6. Conclusions

State-and-transition models of landscape and ecosystem change can potentially represent many modes of environmental change, from simple successional or gradient-driven transitions to complex and (pseudo-) random patterns. Representing STMs as mathematical graphs allows several metrics derived from albegraic graph theory to be applied to assessing modes of landscape change from STMs.

Spectral radius of the adjacency matrix of the STM graph reflects the number and length of cyclic transitions within a landscape, and the extent to which environmental change is likely to be amplified by state transitions. Algebraic connectivity, a measure of network synchronizability, indicates the rate of propagation of state changes through the landscape. The *S*-metric quantifies the extent of system structural constraints to the propagation of state changes. In addition to reflecting different (though related) aspects of STMs, these measures have varying degrees of sensitivity to the number of potential states, the number of possible transitions among states, and the specific arrangement or "wiring" of state transitions.

The case study from the GSARD indicates amplification of changes in system states represented by soil types, relatively rapid spatial propagation of state transitions, and some structural constraints within the system. The implications are that complex, spatially variable state transitions are likely, constrained by local (within-delta) environmental gradients and initial conditions.

The utility of the STM analysis for interpretation of observed environmental change, and to guide choices of specific predictive models, is high. The direct predictive power is relatively low, though the qualitative prediction of modes of change may be quite useful in some cases. However, analysis of other STMs can build insight into the landscape-scale modes of change associated with specific local state transitions.

Acknowledgements

Support for fieldwork in the case study area was provided by a research contract through the Guadalupe-Blanco River Authority. Greg Malstaff of the Texas Water Development Board also provided significant support and encouragement for studies of environmental change in Texas deltaic areas.

References

Anderson, J.B., Rodriguez, A.B. (Eds.), 2008. Response of Upper Gulf Coast Estuaries to Holocene Climate Change and Sea-Level Rise. Geological Society of America Special Paper 443, Boulder, CO.

Bestelmeyer, B.T., Tugel, A.J., Peacock, D.G., Robinett, D.G., Shaver, P.L., Brown, J.R., Herrick, J.E., Sanchez, H., Havstad, K.M., 2009. State-and-transition models for heterogeneous landscapes: a strategy for development and application. Rangeland Ecology and Management 62, 1–15.

Biggs, N., 1994. Algebraic Graph Theory, 2nd ed. Cambridge University Press.

Bode, M., Burrage, K., Possingham, H.P., 2008. Using complex network metrics to predict the persistence of metapopulations with asymmetric connectivity patterns. Ecological Modelling 214, 201–209.

Brierly, G., Fryirs, K., 2005. Geomorphology and River Management. Blackwell, Oxford.

Brinson, M.M., Christian, R.R., Blum, L.K., 1995. Multiple states in the sea-level induced transition from terrestrial forest to estuary. Estuaries 18, 648–659.

Briske, D.D., Fulendor, S.D., Smeins, F.E., 2005. State-and-transition models, thresholds, and rangeland health: a synthesis of ecological concepts and perspectives. Rangeland Ecology and Management 58, 1–10.

Bunn, A.G., Urban, D.L., Keitt, T.H., 2000. Landscape connectivity: a conservation application of graph theory. Journal of Environmental Management 59, 265–278.

Cantwell, M.D., Forman, R.T.T., 1993. Landscape graphs: ecological modeling with graph theory to detect configurations common to diverse landscapes. Landscape Ecology 8, 239–325.

Czembor, C.A., Vesk, P.A., 2009. Incorporating between-expert uncertainty into state-and-transition simulation models for forest restoration. Forest Ecology and Management 259, 165–175.

Donaldson, A.C., Martin, R.H., Kanes, W.H., 1970. Holocene Guadalupe Delta of the Texas Gulf Coast. Deltaic Sedimentation, Modern and Ancient, Society of Economic Paleontologists and Mineralogists Special Publication 15, Tulsa, OK, pp. 107–137.

Duan, Z.-S., Wang, W.-X., Liu, C., Chen, G.-R., 2009. Are networks with more edges easier to synchronize, or not? Chinese Physics B 18, 3122–3130.

Erfanzadeh, R., Garbutt, A., Petillon, J., Maefait, J.P., Hoffmann, M., 2010. Factors affecting the success of early salt-marsh colonizers: seed availability rather than site suitability and dispersal traits. Plant Ecology 206, 335–347.

Fath, B.D., 2007. Structural food web regimes. Ecological Modelling 208, 391–394.

Fath, B.D., Halnes, G., 2007. Cyclic energy pathways in ecological food webs. Ecological Modelling 208, 17–24.

Fath, B.D., Scharler, U.M., Ulanowicz, R.E., Hannon, B., 2007. Ecological network analysis: network construction. Ecological Modelling 208, 49–55.

Gardner, L.H., Porter, D.E., 2001. Stratigraphy and geologic history of a southeastern salt marsh basin, North Inlet, South Carolina, USA. Wetlands Ecology and Management 9, 371–385.

Guckian, W.J., 1986. Soil Survey of Refugio County, Texas. U.S. Department of Agriculture, Natural Resources & Conservation Service.

Hernstrom, M.A., Merzenich, J., Reger, A., Wales, B., 2007. Integrated analysis of landscape management scenarios using state and transition models in the upper Grande Ronde River subbasin, Oregon, USA. Landscape and Urban Planning 80, 198–211.

Li, L., Alderson, D., Doyle, J.C., Willinger, W., 2005. Towards a theory of scale-free graphs: definition, properties, and implications. Technical Report CIT-CDS-04-006, Engineering & Applied Sciences Division, California Institute of Technology, Pasadena, CA, USA. Available from: http://arxiv.org/pdf/cond-mat/0501169.

Miller, W.N., 1982. Soil Survey of Victoria County, Texas. U.S. Department of Agriculture, Natural Resources & Conservation Service.

NRCS (Natural Resources Conservation Service, U.S. Department of Agriculture), 2010. Web Soil Survey. Available from: http://websoilsurvey.nrcs.usda.gov/app/HomePage.htm (last accessed 27.8.10).

Padgaham, M., Webb, J.A., 2010. Multiple structural modifications to dendritic ecological networks produce simple responses. Ecological Modelling 221, 2537–2545.

Phillips, J.D., 1992. Qualitative chaos in geomorphic systems, with an example from wetland response to sea level rise. Journal of Geology 100, 365–374.

Phillips, J.D., in press. Synchronization and scale in geomorphic systems. Geomorphology.

Phillips, J.D., 2010. Changes in Water and Sediment Flow in the San Antonio River Deltaic Plain. Report to the Guadalupe-Blanco River Authority, Seguin, TX.

Restrepo, J.G., Ott, E., Hunt, B.R., 2007. Approximating the largest eigenvalue of network adjacency matrices. Physical Review E, 76, doi:10.1103/PhysRevE.76.056119.

Ricklis, R.A., Blum, M.D., 1997. The geoarchaeological record of Holocene sea level change and human occupation of the Texas gulf coast. Geoarchaeology 12, 287–314.
Soil Survey Division Staff, 1993. Soil survey manual. Soil Conservation Service. U.S. Department of Agriculture Handbook 18.
Thorp, J.H., Thoms, M.C., DeLong, M.D., 2008. The Riverine Ecosystem Synthesis. Academic Press, London.
Tremi, E.A., Halpin, P.N., Urban, D.L., Pratson, L.F., 2008. Modeling population connectivity by ocean currents, a graph-theoretic approach for marine conservation. Landscape Ecology 23, 19–36.
Urban, D.L., Minor, E.S., Tremi, E.A., Schick, R.S., 2009. Graph models of habitat mosaics. Ecology Letters 12, 260–273.
USDA (U.S. Department of Agriculture, Natural Resources Conservation Service), 2010. National Soil Survey Handbook, title 430-VI. Available from: http://soils.usda.gov/technical/handbook (accessed 27.8.10).
van der Wal, R., 2006. Do herbivores cause habitat degradation or vegetation state transition? Evidence from the tundra. Oikos 114, 177–186.
Weistein, R.A., Black, S., 2009. Guadalupe Bay. In Texas Beyond History (online publication), College of Liberal Arts, University of Texas at Austin. Available from: http://www.texasbeyondhistory.net/guadbay/index.html.
Zweig, C.L., Kitchens, W.M., 2009. Multi-state succession in wetlands: a novel use of state and transition models. Ecology 90, 1900–1909.